PROCEEDINGS OF SCIENCE

The Pierre Auger Observatory highlights

Lorenzo Caccianiga[*a] **for the Pierre Auger Collaboration**[b]

[a]*Universitá degli studi di Milano - Italy*
Full author list: http://www.auger.org/archive/authors_2017_09.html
[b]*Av. San Martín Norte 304 (5613) Malargüe, Prov. de Mendoza, Argentina*
E-mail: lorenzo.caccianiga@unimi.it

In the past decade the number of ultra-high energy cosmic rays detected has increased enormously. This is mostly due to the operation of the Pierre Auger Observatory, in Argentina, the largest cosmic ray detector ever built. Through this detector we now know better the most energetic particles in the universe, we can now start to answer some of the most important questions, such as where do they come from? What are they? How do they interact with the atmosphere? In this proceedings a selection of the most important results of Auger are presented, with particular focus on those of astrophysical interest.

XII Multifrequency Behaviour of High Energy Cosmic Sources Workshop
12-17 June
Palermo, Italy

*Speaker.

PoS(MULTIF2017)029

1. The Pierre Auger Observatory

The Pierre Auger Observatory [1], located in Argentina near the town of Malargüe is the largest detector of ultra-high energy cosmic rays (UHECR) ever built. It is a hybrid detector, i.e. it can observe extensive air showers (EAS) induced by the interaction of UHECRs with the atmosphere with independent and complementary instruments: the main two are the fluorescence detector (FD), and the surface detector array (SD). The Observatory has been taking data since 2004 and was completed in 2008. The SD is composed of 1660 water-Cherenkov detectors (WCDs) on a triangular grid of 1500 m spacing (standard array) which covers an area of 3000km^2. In a small area of the array the grid has a denser spacing (750m, infill array) to lower the full efficiency energy threshold, that is 3 EeV [1] for the full array, down to 0.3 EeV. The FD consists of 24 telescopes divided in 4 sites that overlook the area covered by the SD. For FD too an extension to cover lower energies has been deployed: 3 telescopes have been added in the infill region with a higher elevation to look at the showers that develop higher in atmosphere. The FD measures the fluorescence light emitted by the showers as they propagate in the atmosphere, which is proportional to the energy deposited by shower particles, so the FD is capable of performing a calorimetric measurement of the primary cosmic ray energy. However, since it can operate only in clear moonless nights, its duty cycle is limited to $\sim 15\%$. On the other hand, the SD has a 100% duty cycle but can only measure the lateral development of the shower, and cannot measure the primary energy directly. The advantage of a hybrid detector as Auger is that, through the so-called hybrid events, i.e. the events observed by both detectors, it is possible to perform a calibration of the SD and thus compute the energy of SD-only events without the need of simulations. The energy resolution after this process is of the order of 15%. Additional detectors are installed at the observatory site, in particular atmospheric monitors and the AERA array [2] that measures the radio signals emitted by the EAS.

2. Energy Spectrum

One of the main goals of the Pierre Auger Observatory is to measure the cosmic ray spectrum at its highest energy end with unprecedented precision. This is done exploiting all data collected by the observatory, divided into 4 different samples. The SD-1500m and SD-750m samples are made of vertical events (zenith angle $\theta < 60^\circ$ for the standard and $\theta < 55^\circ$ for the infill array) observed by the standard SD array and the infill array respectively. The inclined sample is measured with the standard SD array but covers different zenith angles ($60^\circ < \theta < 80^\circ$) where a different reconstruction is needed, while the hybrid sample is made of events observed by both SD and FD. All the spectra agree within the systematic uncertainties [3], and are combined through a maximum likelihood fit in order to obtain the final spectrum. The latest results show that the spectrum below the *ankle* is well described by a power law with $\gamma_1 = 3.293 \pm 0.002$(stat.) ± 0.05(syst.). The ankle itself is observed at $E_{ankle} = 5.08 \pm 0.06$(stat.)$\pm 0.8$(syst.) EeV and at higher energies the slope of the power law changes to $\gamma_2 = 2.53 \pm 0.02$(stat.)± 0.1(syst.). There is then a strong suppression of the flux, located at $E_s = 39 \pm 0.2$(stat.)± 0.8(syst.) EeV. All these features can be seen in figure 1.

[1] 1 EeV=10^{18} eV

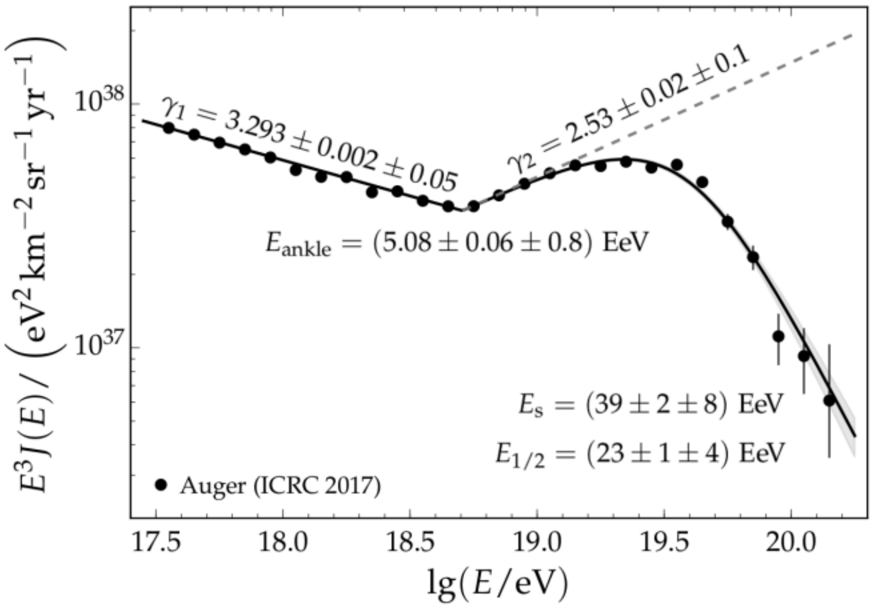

Figure 1: The most up-to date combined spectrum of UHECRs as measured by Auger. The spectral indexes refers to the energy spectrum, here shown multiplied by E^3 to better highlight the spectral features. From [3]

3. Composition

The composition of the UHECR is a key parameter to understand their origin. The best mass-related observable accessible to Auger is X_{max}, i.e. the depth of the maximum of the particle production in the shower, and its second order moment, $\sigma(X_{max})$. Direct measurements of X_{max} can be done only through the FD. The most recent results [4] are shown in figure 2 where the measurements of X_{max} and $\sigma(X_{max})$ as a function of energy are shown.

Information on the mass can be done by comparing the measurements with the prediction from simulations, which however are made based on hadronic interaction models extrapolated from lower energies (the ones accessible with accelerators). Using parametrizations of the expected X_{max} distributions in the hypotesis of a mixed composition with 4 components (p, He, N and Fe) the mass fraction of each component can be inferred. These fractions are shown in figure 3 as a function of energy for different hadronic interaction models. The strong dependence of the results on the hadronic model used is evident, yet we can see that the three models agree when estimating a null Fe abundance between ~ 2 and ~ 25 EeV. Moreover, in all cases an intermediate composition is favored at the highest energies.

4. UHE photons and neutrinos

Auger is capable of observing also showers generated by high-energy photons and neutrinos. The search for such events, and distinguishing them from cosmic-ray ones is not trivial and is carried on with different methods involving both SD and FD. In both cases, no unambiguous detection

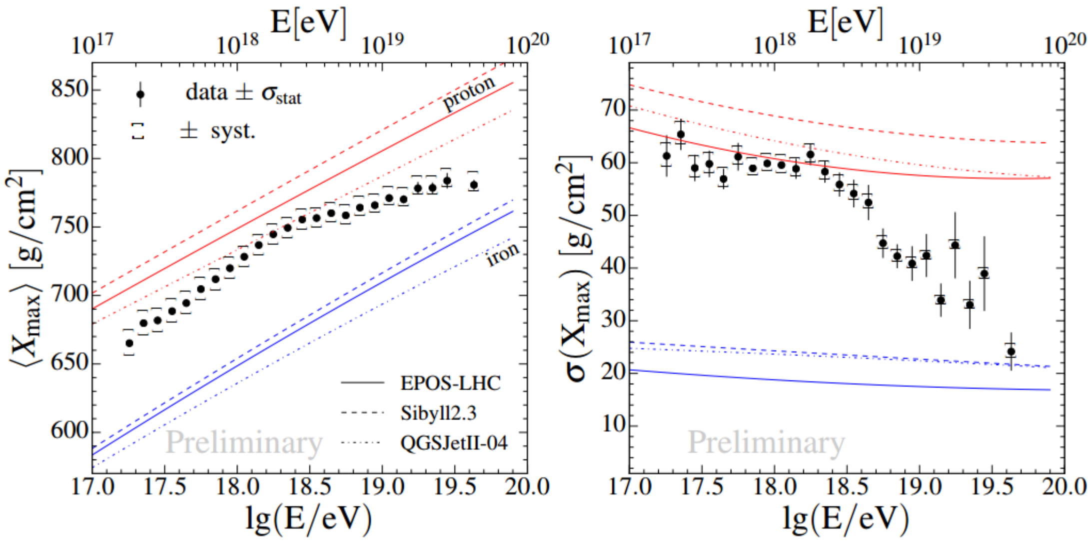

Figure 2: mean X_{max}(left) and $\sigma(X_{max})$ (right) as a function of energy compared to expectations from simulations for proton and iron primaries. From [4]

has been yet performed [5], and stringent upper limits can be placed. Regarding photons, these upper limits severely constrain top-down models for the origin of UHECRs and are now close to reaching the flux expected from GZK photons, i.e. photons produced after a proton CR has interacted with photon background producing a pion and losing energy. A targeted search for HE photons have been performed and this allows to put upper limits in the spectrum of selected targets, such as the Galactic Center as shown in figure 4.

Through neutrino limits, on the other side, constraints can be put on certain sources models [8], particularly those that assume proton primaries and attribute a strong evolution with redshift to the sources. A specific search for neutrino events in coincidence with gravitational waves events GW150914, GW151226, GW170104 and the candidate event LVT151012 has been performed. In the case of GW150914, unfortunately the sky covered by Auger in a short time window from the event did not overlap much with the reconstructed arrival direction region. For the other events, however, a good overlap was found and limits on the energy radiated in UHE neutrinos in the black-hole merging could be placed. An example of the sky overlapping and of the limits put for event GW151226 are shown in figure 5.

5. Arrival directions

The study of the arrival directions of UHECRs is perhaps the most natural way to try and infer their sources. However, since cosmic rays are charged particles, this is made difficult because of the deflections they go through when passing through the Galactic and extragalactic magnetic fields. The precise magnitude and direction of these fields is unknown but the deflections are thought to be of the order of few degrees for a proton at 100 EeV in most parts of the GMF [11]. Because of this, one can either look at the highest energies, where deflection should be the least, and search

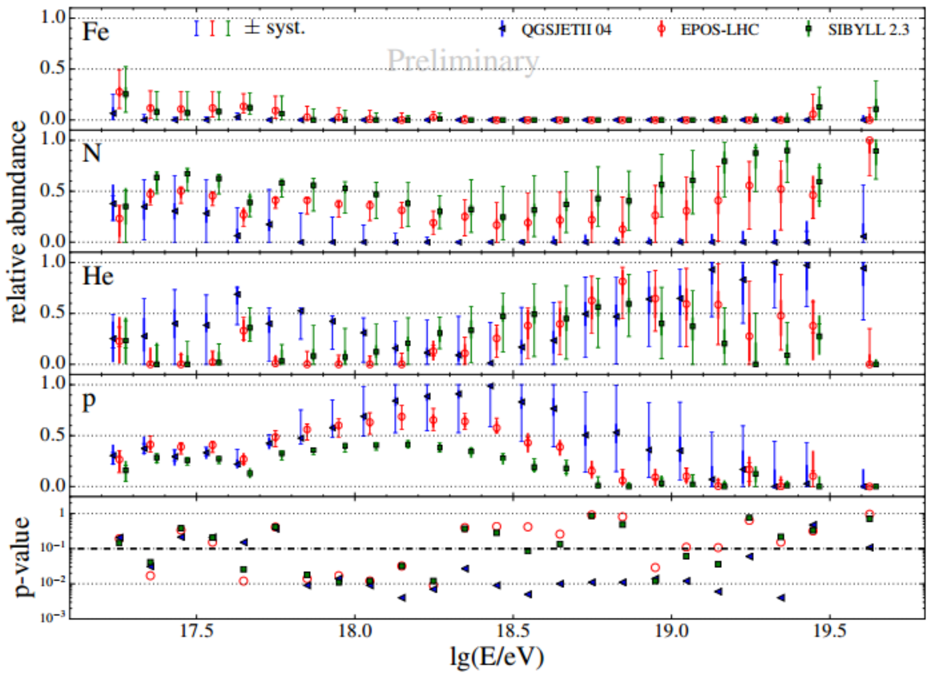

Figure 3: Mass fraction fits obtained using parametrizations of the expected X_{max} distributions. The error bars indicate the statistics (smaller cap) and the systematic uncertainties (larger cap). The bottom panel indicates the goodness of the fits (p-values). From [4]

for small and intermediate scale anisotropies or look also at lower energies looking for large scale anisotropies. The Pierre Auger Observatory has recently [12] observed a large scale anisotropy for the events with energy greater than 8 EeV. In this energy range, through a Rayleigh analysis in right ascension, the amplitude of the first harmonic was found to be incompatible with expectations from an isotropic distribution at more than 5.2 σ level. On the other hand, the same analysis on lower energy events (4-8 EeV) lead to a result compatible with isotropy. The direction of the reconstructed dipole in the high energy bin lies $\sim 125°$ from the galactic center. This suggests an extragalactic origin of such anisotropy and, because of Liouville's theorem, the distribution of cosmic rays must also be anisotropic outside of the Galaxy, since the anisotropy cannot arise through deflections of an originally isotropic flux by a magnetic field. An extragalactic origin of cosmic rays is favored also in the 4-8 EeV energy bin, where anisotropy was expected if the sources were distributed on the Galactic plane. The tension between the constraints on the dipole amplitude and the Galactic origin scenarios could be alleviated in case of an heavy composition of cosmic rays in this energy range, however this is disfavored by composition measurements that favor light primaries at these energies (see section 3).

Auger has published in 2015 an extensive search for small and intermediate-scale anisotropies with data up to 30 March 2014 [13]. These searches were performed by counting the number of couples UHECR-candidate sources separated by less than a certain angular distance ψ. This number was then compared to the one expected from an isotropic distribution of UHECRs and a scan on ψ and other quantities (minimum energy of UHECRs, maximum distance of candidate

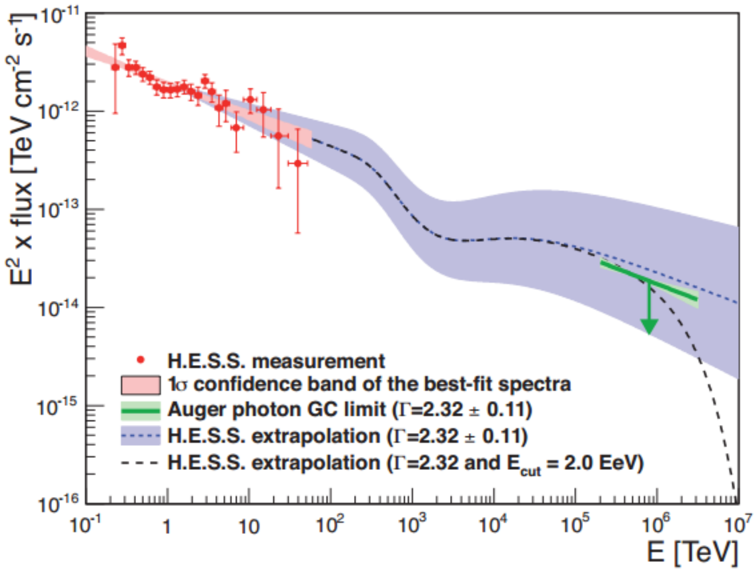

Figure 4: γ spectrum of the Galactic center region. The flux measured by H.E.S.S. in the TeV range [6] is shown in red, as well as the extrapolation to the EeV range (blue dashed line). The upper limit on the flux derived in the analysis presented here is given in green. A spectrum with an exponential cutoff at 2 EeV is shown as the black dashed line. From [7]

sources, minimum luminosity of candidate sources) was performed in order to find the most significant excess from isotropy. Among these searches, the most significant findings were a hint of correlation with bright AGN observed by *Swift* (penalized P-value: 1.3%, $\psi = 18°$, $E_{th} = 58$ EeV, $D_{max} = 130$ Mpc , $L_{min} = 10^{44} erg/s$) and an hint of excess in the direction of Centaurus A, the closest radiogalaxy (penalized P-value: 1.4%, $\psi = 15°$, $E_{th} = 58$ EeV). These numbers where recently updated [14] with data up to 30 April 2017 with an updated energy scale, finding the excess with *Swift* AGN to be at $\psi = 16°$, $E_{th} = 62$ EeV, $D_{max} = 130$ Mpc , $L_{min} = 10^{44} erg/s$ with a post-trial P-value of $6.5 \cdot 10^{-4}$ (3.2 σ) and the excess with Cen A to be at the same position as before with a post-trial P-value of $1.1 \cdot 10^{-3}$.

A different type of analysis has been also performed, based on the assumption that the UHECR flux is proportional to the non-thermal electromagnetic flux. This analysis then takes into account the different flux of the single candidate sources, that in the previous analysis were all weighted equally. For this studies, two different candidate sources were taken into account: AGNs and starburst (starforming) galaxies. Active galaxies were extracted from the *Fermi*-LAT 2FHL Catalog [15], selecting only radio-loud AGNs within a 250 Mpc radius. A list of 17 bright nearby candidates was obtained this way, and their integral γ-ray fluxes between 50 GeV and 2 TeV were used as a proxy for the UHECR flux. For starburst galaxies, since only a few of them were observed directly in the γ-ray band, the informations from *Fermi*-LAT were supplemented with observations in the radio band, since γ-ray luminosity has been shown to nearly linearly scale with radio flux [16]. Continuum emission at 1.4 GHz was then used as a proxy for the UHECR flux. This way the 23 brightest nearby objects with a radio flux larger than 0.3 Jy were selected. In order to take into

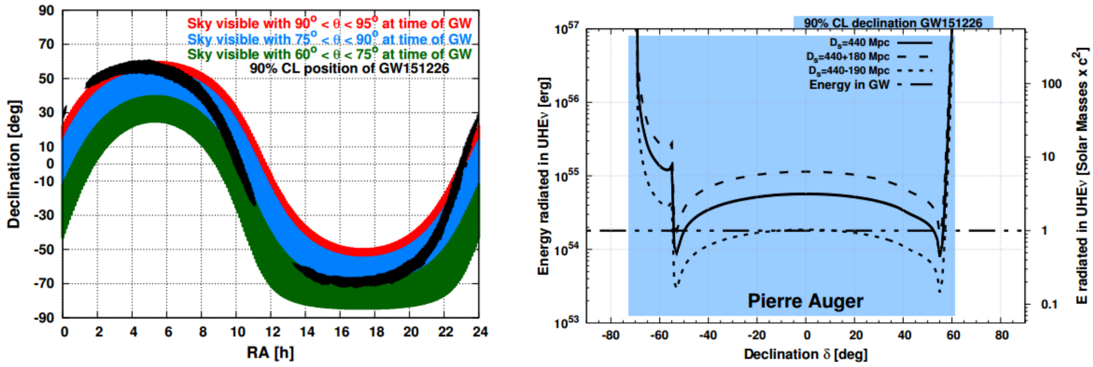

Figure 5: Left: Auger sky coverage at different zenith angles at the time of the detection of GW151226. The black contour region corresponds to the 90 % C.L. region for the GW event location. Right: Constraints on the radiated energy in UHE neutrinos (per flavor) from the source of GW151226 as a function of declination. Energies above the solid line are excluded at the 90% C.L. The calculation is done for a distance Ds = 410 Mpc (dashed lines correspond to reported distances at the 90% C.L.). The dot-dashed horizontal line represents, the inferred energy radiated in gravitational waves for that event [9]. The shaded region indicates the 90% C.L. region for the GW event location. From [10]

account the flux of the single sources, a different analysis method is needed: a maximum likelihood method was used comparing a probability map of the arrival distribution of cosmic rays obtained from the candidate sources distribution to the observed distribution of events using an appropriate test statistic (TS). The first map is obtained by smearing the sources position through a Fisher-Von Mises distribution and weighting each source based on its flux. The weights also take into account the distance of the object, to take into account the propagation effects in the intergalactic medium. The angular smearing applied to each source is the first of the two free parameters in this analysis and acts as an effective search radius taking into account the unknown deflections of the UHECRs in the magnetic fields. The second free parameters is the isotropic fraction, [2] i.e. the weight of an isotropically distributed map that is added to the probability map to take into account a diffuse component of UHECR. The likelihood function (L) is then given by the product over the events of the probability map. The test statistics is calculated as $TS = 2\ln L/L_0$ where L_0 is the likelihood for an isotropic distribution of UHECRs, that here acts as *null hypotesis*. The TS is then maximized as a function of two free parameters in different energy threshold from 20 up to 80 EeV. In Figure 6, the TS as a function of the two free parameters is reported for the energy threshold where the maximum is found: 60 EeV for the AGNs and 39 EeV for the starburst galaxies. The best-fit parameters are found to be a smearing angle of 13° and an anisotropic fraction of 10% for the starburst-galaxies with a TS of 24.9, corresponding to a significance of $\sim 4\sigma$, and 7° and 7% for the γ-ray AGNs with a TS of 15.2 corresponding to a significance of $\sim 2.7\sigma$. It is possible to see that while the significance for the AGNs is close to the one obtained with the previous analysis, a much higher significance is obtained with the newly tested starburst hypotesis.

[2] Actually, in the following will rather be reported the *anisotropic* fraction, defined as $1 - f_{iso}$.

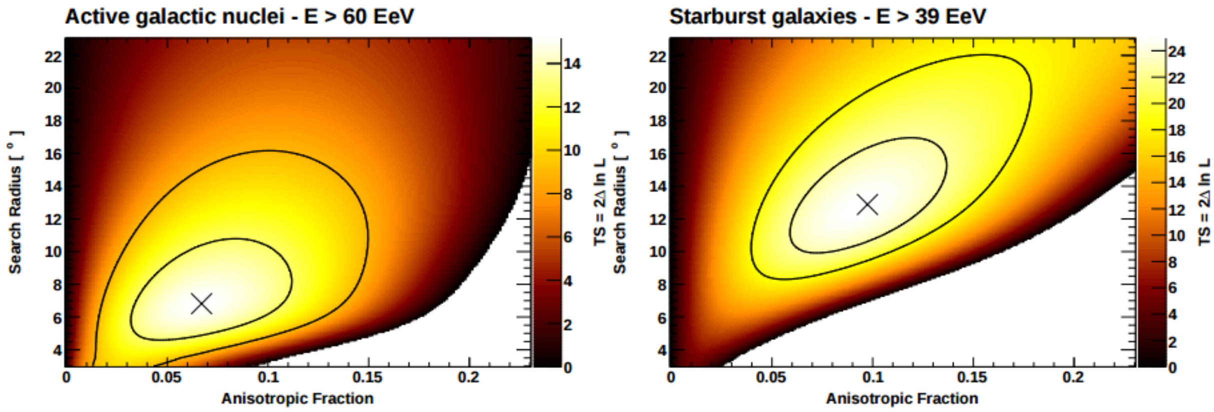

Figure 6: Test statistic as a function of the smearing angle and anisotropic fraction for the best fit energy for the AGNs (left panel) and for the starburst galaxies (right panel). The solid lines indicate the 1 and 2 σ confidence contours. From [14]

6. Auger Prime: the Auger upgrade

We have seen that the UHECR mass composition is a key parameter and that, at the highest energies, it cannot at present be well determined. For this reason, the Collaboration is now working on a major upgrade of the detector, called *Auger Prime* [17]. A number of improvement are foreseen for this upgrade that should lead Auger data acquisition to last at least until 2025. The most important of them is the deployment of plastic scintillators of approximate area of $\sim 4\text{m}^2$ on top of each SD station (SSD). The two detectors will respond differently to the electromagnetic and muonic components of the showers, and by comparison of the signal in each of them a direct estimation of the muonic signal can be computed. A small portion of the array will benefit also from buried muon detectors that can calibrate and validate the measurements made with the SSD. In addition to that, each SD station will be equipped with a faster electronics and a new PMT, much smaller than the existing ones, to improve the station dynamic range. On the FD side, the up time will be extended to partially moon-illuminated nights by decreasing the gain of the PMTs in the FD cameras. At present, the upgrade is in pre-production phase and prototypes detectors are already in the field and taking data.

7. Conclusions and outlook

The past decade has been enormously important in the UHECR physics: thanks in particular to the Pierre Auger Observatory, the flux of those particles, the characteristics of the air showers they induce and, within certain limits, their composition are now known up to an unprecedented level. These very days, important results are being published also regarding the arrival direction of the highest-energy cosmic rays. Still, there is lots of work to be done: the astrophysical sources of these particles, the most energetic known in the universe, are unknown. A better understanding of this and other open questions will be strongly supported by Auger upgrade, Auger Prime, that will allow for a better understanding of the composition at the highest energies. We hope that the next decade will be as important for this fields as the past one.

References

[1] The Pierre Auger Collaboration, *The Pierre Auger Cosmic Ray Observatory*, *Nuclear Instruments and Methods in Physics Research Section A: Accelerators, Spectrometers, Detectors and Associated Equipment* (2015) .

[2] The Pierre Auger Collaboration, *Energy estimation of cosmic rays with the Engineering Radio Array of the Pierre Auger Observatory*, *Physical Review D* **93** (2016) 122005.

[3] F. Fenu for The Pierre Auger Collaboration, *The cosmic ray energy spectrum measured by the Pierre Auger Observatory*, 2017.

[4] J. Bellido for The Pierre Auger Collaboration, *Depth of maximum of air-shower profiles at the Pierre Auger Observatory: Measurements and composition implications*, 2017.

[5] M. Niechciol for The Pierre Auger Collaboration, *Diffuse and targeted searches for ultra-high-energy photons using the hybrid detector of the Pierre Auger Observatory*, 2017.

[6] The HESS Collaboration, *Acceleration of petaelectronvolt protons in the Galactic Centre*, *Nature* **531** (2016) 476âĂŞ479.

[7] The Pierre Auger Collaboration, *A targeted search for point sources of EeV photons with the Pierre Auger Observatory*, *The Astrophysical Journal Letters* **837** (2017) L25.

[8] E. Zas for The Pierre Auger Collaboration, *Searches for neutrino fluxes in the EeV regime with the Pierre Auger Observatory*, 2017.

[9] B. Abbott, R. Abbott, T. Abbott, M. Abernathy, F. Acernese, K. Ackley et al., *GW151226: Observation of gravitational waves from a 22-solar-mass binary black hole coalescence*, *Physical Review Letters* **116** (2016) 241103.

[10] The Pierre Auger Collaboration, *Ultrahigh-energy neutrino follow-up of gravitational wave events GW150914 and GW151226 with the Pierre Auger Observatory*, *Physical Review D* **94** (2016) 122007.

[11] R. Jansson and G. R. Farrar, *A New Model of the Galactic Magnetic Field*, *The Astrophysical Journal* **757** (2012) 14, [1204.3662].

[12] The Pierre Auger Collaboration, *Observation of a large-scale anisotropy in the arrival directions of cosmic rays above 8*$\times 10^{18}$ *eV*, *Science* **357** (2017) 1266–1270.

[13] The Pierre Auger Collaboration, *Searches for anisotropies in the arrival directions of the highest energy cosmic rays detected by the Pierre Auger Observatory*, *The Astrophysical Journal* **804** (2015) 15.

[14] U. Giaccari for The Pierre Auger Collaboration, *Arrival directions of the highest-energy cosmic rays detected by the Pierre Auger Observatory*, 2017.

[15] M. Ackermann, M. Ajello, W. Atwood, L. Baldini, J. Ballet, G. Barbiellini et al., *2FHL: the second catalog of hard Fermi-LAT sources*, *The Astrophysical Journal Supplement Series* **222** (2016) 5.

[16] M. Ackermann, M. Ajello, A. Allafort, L. Baldini, J. Ballet, D. Bastieri et al., *GeV observations of star-forming galaxies with the Fermi Large Area Telescope*, *The Astrophysical Journal* **755** (2012) 164.

[17] The Pierre Auger Collaboration, *The Pierre Auger Observatory Upgrade Preliminary Design Report*, *arXiv:1604.03637* .